

Lagrangian statistics in the central North Pacific

Rick Lumpkin^{a,b,*}, Pierre Flament^{a,b}

^a *University of Hawaii at Manoa, Honolulu, HI, USA*

^b *IFREMER, Plouzané, France*

Received 6 December 1999; accepted 3 June 2000

Abstract

Lagrangian integral scales, diffusivities, dispersion and velocity spectra are calculated using surface drifter trajectories in the central North Pacific. The meridional integral time scale is relatively homogeneous throughout the region; a large increase in the zonal time and length scales south of Hawaii is attributed to meanders in the North Equatorial Current. Except in this current, the initial dispersion is consistent with Taylor's Theorem. For lags of 20–120 days, the meridional dispersion can be modeled by a constant eddy diffusivity. Shear in the mean zonal currents magnifies the zonal dispersion at long lags. In the Lagrangian spectra, the energetic eddy band is at 3–20 days west of Hawaii, 10–40 days east and north of Hawaii, and 20–60 days in the North Equatorial Current. In the wake of Hawaii, energetic lee vortices produce sharp peaks in the cyclonic and anticyclonic rotary spectra. © 2001 Elsevier Science B.V. All rights reserved.

Keywords: Diffusivities; North Pacific; Eddy

1. Introduction

The gyre-scale motion of the central North Pacific Ocean consists of the eastward North Pacific Current and the westward North Equatorial Current (NEC). The Hawaiian Islands lie near the northern extent of the NEC, partially blocking it. West of the islands, energetic mesoscale lee vortices dominate the instantaneous currents and have profound effects on the time-averaged flow field (Patzert, 1969; Lumpkin, 1998; Flament et al., 2001). Over the last decade, these currents and vortices have been sampled by WOCE/SVP drifting buoys (Fig. 1). Single-particle Lagrangian integral scales, which give the dominant

stirring scales of oceanic turbulence, can be calculated from their trajectories. Classical diffusion theory relates these integral scales to the long-term dispersion in terms of an eddy diffusivity. However, this parameterization requires stationary and homogeneous currents, while oceanic drifters experience inhomogeneous mean currents and a mesoscale field which changes in both space and time. As a consequence, Freeland et al. (1975) concluded that even the short-time dispersion of deep, neutrally buoyant floats cannot be described by classical theory. Subsequent drifter studies (cf. Colin de Verdière, 1983; Krauss and Böning, 1987; Paduan and Niiler, 1993) have not found this inconsistency, although at longer times the dispersion may not asymptote to the diffusive limit of classical theory.

In this paper, we present the Lagrangian statistics of surface drifters in the central North Pacific. In Section 2, a brief review of classical diffusion theory

* Corresponding author. Department of Oceanography, Florida State University, 329 OSB, West Call St., Tallahassee, FL 32306-4320, USA. Tel.: +1-850-644-1987; fax: +1-850-644-2581.

E-mail address: rlumpkin@ocean.ocean.fsu.edu (R. Lumpkin).

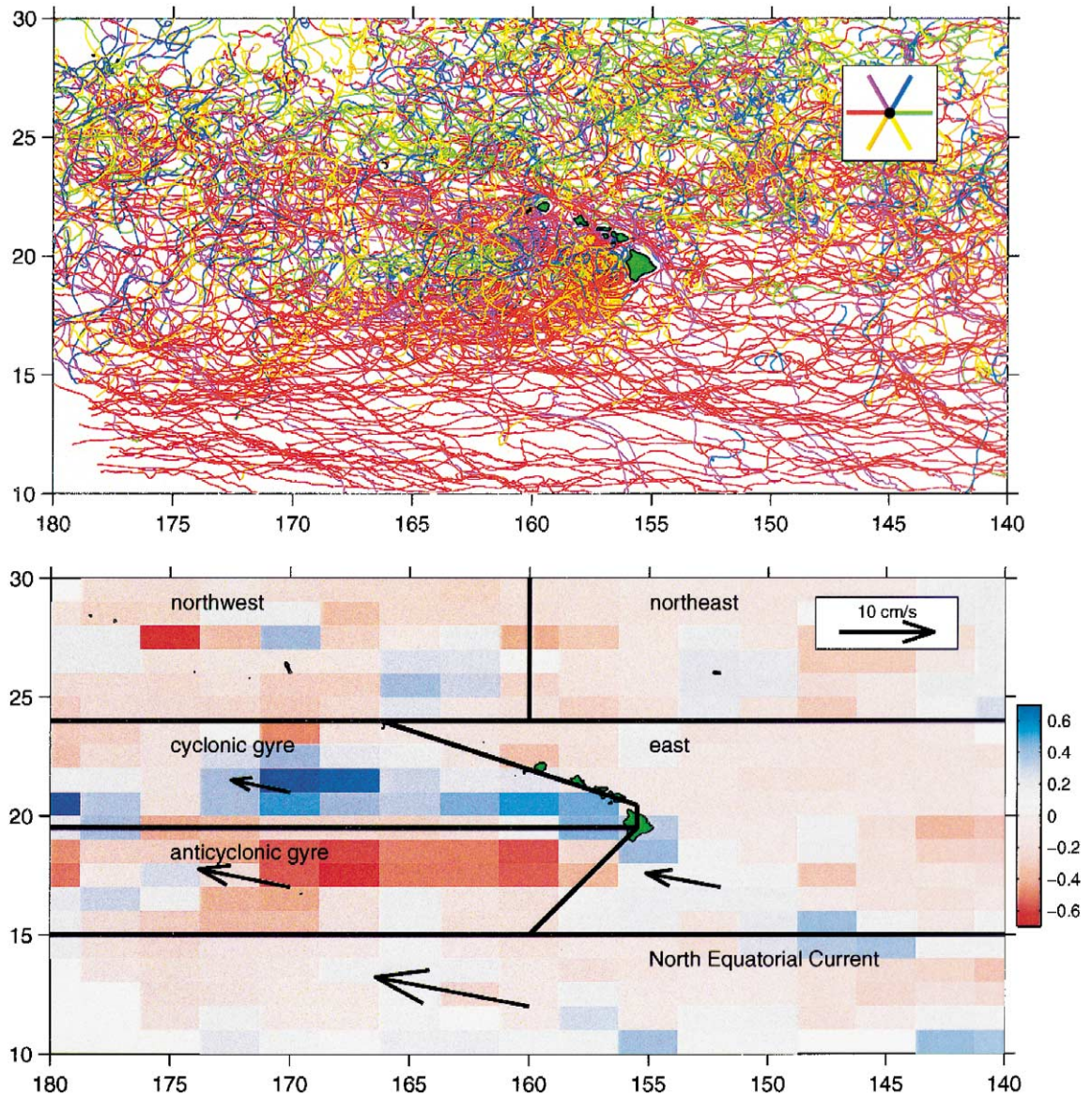


Fig. 1. Top: Spaghetti diagram of 20-day drifter trajectory segments. Colors give the mean drift direction (legend in upper-right corner). Bottom: Map of vorticity created from the spectra of 90-day drifter segments. Blue indicates predominantly cyclonic vorticity, red indicates anticyclonic vorticity. Black polygons indicate the drifter group subregions. Arrows show the mean velocity of the drifter group.

is presented. Section 3 describes the drifter database and integral scale calculations, and presents these scales for several groups of drifters. In Section 4, the diffusion model's predictions are compared to the directly observed dispersion of the drifters. It is shown that the meridional dispersion agrees with

classical theory, but the zonal dispersion is greatly magnified. Section 5 examines the hypothesis that this magnification is due to meridional shear in the mean zonal currents. The Lagrangian spectra are examined for significant zonal/meridional and rotary motion in Section 6. Section 7 concludes by

examining the relevance of an empirical law which relates length and time scales to characteristic eddy speeds.

2. Classical diffusion theory

Consider a cloud of particles released into a fluid at a single point. The instantaneous current $u(t)$ experienced by a particle can be divided into a mean component u_o (identical for all particles), and a fluctuating component $u'(t)$ (which may vary from one particle to the next). The position of an individual particle in the cloud is $x(t) = u_o t + x'(t)$, where

$$x' = \int_0^t d\tau u'(\tau). \quad (1)$$

Dispersion is $\langle x'^2 \rangle$, where the brackets denote an average over the particle ensemble. Assuming that u' is ergodic, Eq. (1) can be used to derive Taylor's Theorem (Taylor, 1921):

$$\langle x'^2 \rangle = 2u_{\text{rms}}^2 \int_0^t d\tau (t - \tau) R_u(\tau), \quad (2)$$

where $u_{\text{rms}} \equiv \sqrt{\langle u'^2 \rangle}$ and the autocorrelation function R_u is

$$R_u(\tau) = \lim_{T_m \rightarrow \infty} \frac{1}{u_{\text{rms}}^2 T_m} \int_0^{T_m} dt u'(t) u'(t + \tau). \quad (3)$$

The characteristic time scale of dispersion is the Lagrangian integral time

$$T_u = \int_0^\infty d\tau R_u. \quad (4)$$

It can be combined with the eddy speed urms to derive the Lagrangian integral length $L_u = u_{\text{rms}} T_u$. At short times, $R_u \approx 1$ and the dispersion is

$$\langle x'^2 \rangle \approx u_{\text{rms}}^2 t^2 \quad (t \ll T_u) \quad (\text{ballistic regime}). \quad (5)$$

In this short-time limit, the rms particle displacement increases linearly with time, with a slope equal to the rms eddy speed. At large times,

$$\langle x'^2 \rangle \approx 2u_{\text{rms}}^2 T_u t \quad (t \gg T_u) \quad (\text{random-walk regime}), \quad (6)$$

assuming that the integral in Eq. (4) converges. The rms particle displacement slows from the initial rate ($\propto t$) to a random-walk ($\propto \sqrt{t}$).

By analogy with Fickian diffusion, dispersion can be parameterized as an eddy diffusivity K_{xx} (Taylor, 1921; Batchelor, 1949; Davis, 1982):

$$K_{xx} = \frac{1}{2} \frac{d}{dt} \langle x'^2 \rangle. \quad (7)$$

From Eq. (6), the diffusivity asymptotes to

$$K_{xx} = u_{\text{rms}}^2 T_u, \quad (8)$$

in the random walk regime $t \gg T_u$ (again, assuming homogeneity and stationarity for u').

3. Integral scales in the central North Pacific

A total of 356 WOCE/SVP surface drifters have been deployed in or passed through the central North Pacific (10–30°N, 140–180°W). Raw satellite fixes of drifter position were quality-checked using a two-step scheme and interpolated to 1/4-day intervals via kriging (Hansen and Poulain, 1996). The interpolated data span 286 drifter-years (Fig. 1). West of the Hawaiian Islands, many cycloidal trajectories are created by drifters orbiting westward-propagating lee vortices. This westward motion is visible on either side of 19.5°N along 155–170°W. At 19.5°N, a narrow band of eastward drift (colored green in Fig. 1) marks the Hawaiian Lee Countercurrent (Lumpkin, 1998). South of the islands, the mean westward NEC dominates the trajectories, which also display zonally extended meridional fluctuations. East and north of the islands, the trajectories are a mix of loops and wiggles with no visually discernible mean drift.

After formation immediately west of Hawaii, lee vortices drift westward due to the β -effect and advection by the North Equatorial Current. Because anticyclonic eddies tend to drift southward while cyclonic eddies drift northward (Chassignet and Cushman-Roisin, 1991), the overall field of lee eddies is not random; instead, it is organized in a pattern superficially resembling a Kármán vortex street (Lumpkin, 1998). Rectification of this field may produce the elongated, counter-rotating lee gyres which extend for over 1000 km west of the islands in the time-averaged currents (Lumpkin, 1998; Flament et al., 2001). The vorticity structure of this geophysical-scale wake can be seen by breaking the drifter trajectories into 90-day nonoverlapping segments,

calculating the mean rotary spectra in $3 \times 1^\circ$ cells, and integrating the spectra over subinertial frequen-

cies to obtain the cyclonic and anticyclonic variance. Fig. 1 shows the resulting map of cyclonic/total

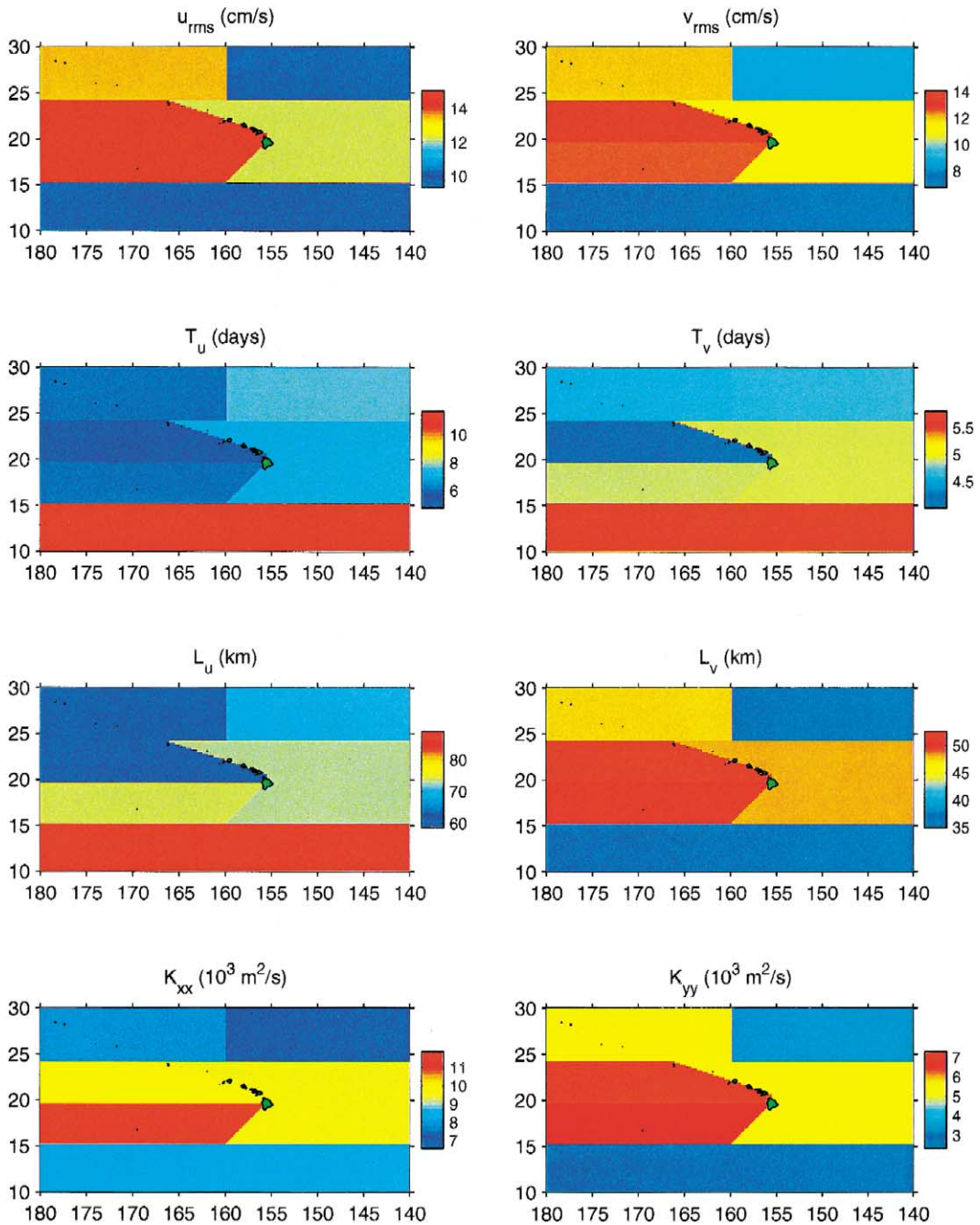


Fig. 2. Top: zonal (left) and meridional (right) rms eddy speed (cm/s). Middle, upper: Lagrangian zonal (left) and meridional (right) time scales (days). Middle, lower: Lagrangian zonal (left) and meridional (right) length scales (km). Bottom: Zonal (left) and meridional (right) eddy diffusivities ($10^3 \text{ m}^2/\text{s}$).

variance, scaled from +1 (purely cyclonic) to -1 (purely anticyclonic). In the lee gyres, as much as 70% of the variance is of one sign; the division between the cyclonic and anticyclonic gyre is at 19.5°N, the latitude of the eastward Hawaiian Lee Countercurrent.

In order to calculate Lagrangian statistics for the various dynamically homogeneous regions, the 90-day trajectory segments were organized into six groups according to their median latitude and longitude (Fig. 1). For each segment within a group, the ensemble-averaged velocity was removed from the drifter-derived velocities. Because direct estimates of the autocorrelation function R are contaminated by noise and uncertainties in the mean current, and this contamination dominates R at large lags, the integration in Eq. (4) was truncated at the first zero crossing of R (cf. (Freeland et al., 1975; Krauss and Böning, 1987; Poulain and Niiler, 1989)).

The mean scales of the six groups are shown in Fig. 2 and listed in Table 1. The lee gyres and northwest groups have the highest eddy kinetic energy levels, while the North Equatorial Current and

northeast groups have the lowest. The rms eddy speeds for all groups except the cyclonic gyre are significantly anisotropic, with zonal speeds exceeding meridional speeds by a factor of 1.1–1.4. In the cyclonic gyre, where the maximum eddy kinetic energy levels are found, the ratio is not significantly different from unity. For the five groups north of the North Equatorial Current, the time scales are quite homogeneous, with an overall mean of $(T_u, T_v) = (6.3 \pm 0.5, 4.6 \pm 0.2)$ days. The smallest time scales are in the cyclonic gyre, where drifters advect rapidly around lee vortices. The overall mean length scale of these five groups is $(L_u, L_v) = (68 \pm 3, 46 \pm 3)$ km. Perhaps the most striking feature of Fig. 2 is the much larger zonal time and length scales in the North Equatorial Current. These large scales suggest that low-frequency, zonally extended meanders (rather than more isotropic, higher-frequency mesoscale vortices) dominate the variability here (Krauss and Böning, 1987). Eddy diffusivities were calculated using Eq. (8), and range from 11.9×10^3 m²/s in the eddy-rich anticyclonic gyre to 2.3×10^3 m²/s in the North Equatorial Current.

Table 1
Lagrangian integral scales in each group, calculated from independent 90-day segments

Northwest (31.2 drifter years)	$(u_{\text{rms}}; v_{\text{rms}}) = (13.5 \pm 0.5, 12.0 \pm 0.4)$ cm/s $(T_u; T_v) = (6.1 \pm 0.4, 4.6 \pm 0.5)$ days $(L_u; L_v) = (64 \pm 7, 47 \pm 4)$ km $(K_{xx}; K_{yy}) = (7.9 \pm 1.3, 5.6 \pm 0.5) \times 10^3$ m ² /s
Cyclonic gyre (35.8 drifter years)	$(u_{\text{rms}}; v_{\text{rms}}) = (15.1 \pm 0.5, 14.1 \pm 0.5)$ cm/s $(T_u; T_v) = (4.8 \pm 0.4, 4.0 \pm 0.4)$ days $(L_u; L_v) = (58 \pm 7, 53 \pm 5)$ km $(K_{xx}; K_{yy}) = (9.6 \pm 1.1, 7.3 \pm 0.6) \times 10^3$ m ² /s
Anticyclonic gyre (32.2 drifter years)	$(u_{\text{rms}}; v_{\text{rms}}) = (15.0 \pm 0.8, 12.5 \pm 0.5)$ cm/s $(T_u; T_v) = (6.1 \pm 0.6, 4.9 \pm 0.3)$ days $(L_u; L_v) = (74 \pm 6, 49 \pm 3)$ km $(K_{xx}; K_{yy}) = (11.9 \pm 1.3, 6.6 \pm 0.4) \times 10^3$ m ² /s
Northeast (58.8 drifter years)	$(u_{\text{rms}}; v_{\text{rms}}) = (10.3 \pm 0.4, 8.9 \pm 0.4)$ cm/s $(T_u; T_v) = (7.6 \pm 0.5, 4.7 \pm 0.2)$ days $(L_u; L_v) = (69 \pm 4, 35 \pm 3)$ km $(K_{xx}; K_{yy}) = (6.6 \pm 0.5, 3.3 \pm 0.2) \times 10^3$ m ² /s
East (72.3 drifter years)	$(u_{\text{rms}}; v_{\text{rms}}) = (12.2 \pm 0.3, 11.1 \pm 0.3)$ cm/s $(T_u; T_v) = (7.1 \pm 0.4, 4.9 \pm 0.3)$ days $(L_u; L_v) = (73 \pm 6, 48 \pm 2)$ km $(K_{xx}; K_{yy}) = (9.5 \pm 0.7, 5.4 \pm 0.3) \times 10^3$ m ² /s
North equatorial current (28.9 drifter years)	$(u_{\text{rms}}; v_{\text{rms}}) = (9.3 \pm 0.6, 6.7 \pm 0.2)$ cm/s $(T_u; T_v) = (11.7 \pm 0.9, 5.8 \pm 0.5)$ days $(L_u; L_v) = (89 \pm 9, 35 \pm 3)$ km $(K_{xx}; K_{yy}) = (8.2 \pm 1.1, 2.3 \pm 0.2) \times 10^3$ m ² /s

Fig. 3 shows the zonal and meridional scales and diffusivities as functions of the rms eddy speed. For comparison, data are included from Colin de Verdière (1983) (eastern North Atlantic, 47°N, 11°W), Krauss and Böning (1987) (central North Atlantic from 30°N to 55°N), and Poulain and Niiler (1989) (southern California Current System). Except for the North Equatorial Current values, the central North Pacific scales are consistent with the central North Atlantic values for a given rms eddy speed, suggesting that the underlying Eulerian length and time scales of the mesoscale fluctuations are similar. The North Equatorial Current group was further south than any drifters in the North Atlantic study; thus, the discrepancy in Lagrangian zonal length scales, and the much smaller length scales found by Colin de Verdière at 47°N, may be caused by an Eulerian length scale which decreases with increasing latitude (Stammer, 1997). The central North Pacific meridional

ional scales are also consistent with those in the California Current; the inconsistency in zonal scales between these studies may be due to the influence of the North American coast.

4. Asymptotic behavior of the dispersion

Is the dispersion consistent with Taylor's Theorem? To address this, we divided the trajectories into 120-day segments and resampled the tracks every 10 days, treating each segment as independent (Freeland et al., 1975; Poulain and Niiler, 1989). Fig. 4 shows the rms displacement of the drifter groups, with the ballistic growth rate (Eq. (5)) given by the rms eddy speeds. Everywhere except in the North Equatorial Current, the initial growth is consistent with Taylor's Theorem. Zonal dispersion in the NEC is faster than ballistic, growing instead at $\sim (14.6 \text{ cm/s})t$.

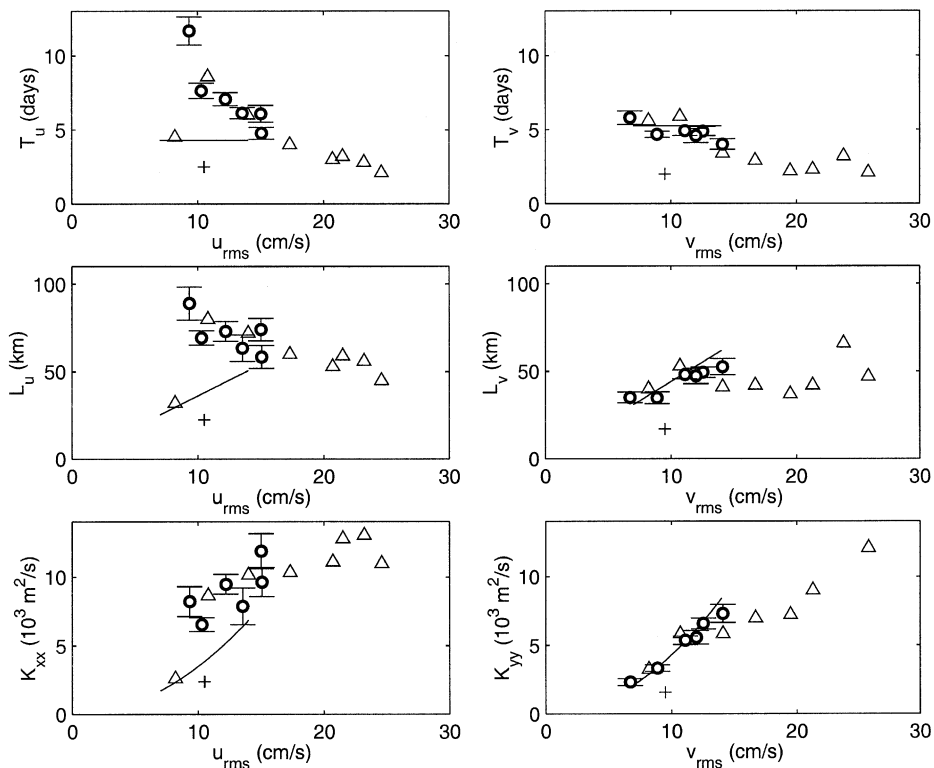


Fig. 3. Lagrangian properties as a function of rms eddy speed (left: zonal, right: meridional). Circles with standard error bars are the central North Pacific values. For comparison, triangles give values from Krauss and Böning (1987), pluses from Colin de Verdière (1983), and solid lines from Poulain and Niiler (1989) (their least-squares fits to a cloud of values).

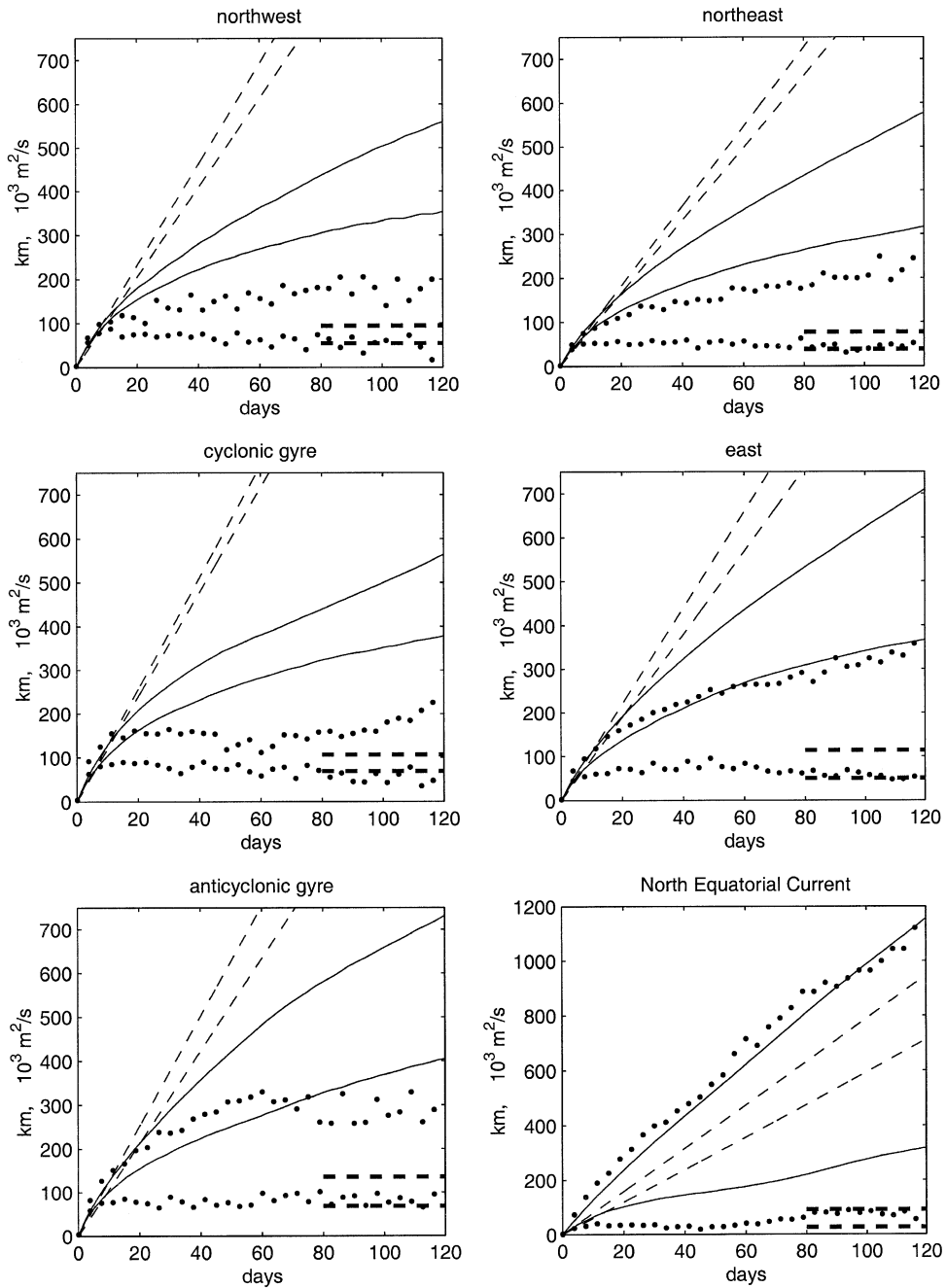


Fig. 4. Dispersion and diffusivity for the six drifter groups. In all cases, the upper curve is zonal and the lower is meridional. Solid lines: rms displacement (km). Thin dashed lines: ballistic rms displacement according to rms eddy speed (km). Dots: eddy diffusivity calculated via Eq. (7) ($10^3 \text{ m}^2/\text{s}$). Heavy dashed lines: random-walk diffusivity limit predicted by Eq. (8) ($10^3 \text{ m}^2/\text{s}$).

If the drifters enter the random-walk regime at long times, the eddy diffusivity should approach a

constant. Fig. 4 shows the diffusivity calculated via Eq. (7) and low-passed at 15 days, with heavy

dashed lines indicating the limit predicted by Eq. (8). For all groups, meridional diffusivity reaches the predicted value by day 20, with slight fluctuations thereafter. Taylor's Theorem does not describe the zonal dispersion of any group. In the cyclonic gyre, drifters disperse zonally like a random walk in days 15–100, with an apparent diffusivity 1.5 times greater than predicted by the integral scales, but beyond day 100 the rms displacement resumes linear growth. In contrast, the anticyclonic gyre group takes much longer to settle into random-walk dispersion (60 days), but remains random-walk-like to day 120. For all other groups, the zonal dispersion never acts like a random walk; instead, rms displacement switches from the linear ballistic rate (except for the NEC group) to a smaller, but still linear, growth rate through day 120, with the diffusivity according to Eq. (7) continuously increasing.

5. Shear dispersion

The long-time linear growth in zonal rms displacement is consistent with dispersion driven by shear in the mean zonal currents. To demonstrate this, consider mean currents of the form

$$\langle u \rangle = u_o + \alpha y', \quad \langle v \rangle = 0, \quad (9)$$

(see Appendix of Krauss and Böning (1987)). A spatially homogeneous estimate of $\langle u \rangle$ will be averaged over a meridional scale B (the maximum meridional size of the tracer cloud). This estimate, denoted with a hat, is

$$\langle \hat{u} \rangle = \frac{1}{B} \int_{-B/2}^{B/2} dy' \langle u \rangle = u_o. \quad (10)$$

The estimate of u' is, thus, contaminated by the meridional shear of the mean current:

$$\hat{u}' = u - \langle \hat{u} \rangle = u_o + \alpha y' + u' - u_o = u' + \alpha y'. \quad (11)$$

Then

$$\langle \hat{u}'^2 \rangle = \langle u'^2 \rangle + 2\alpha \langle u' y' \rangle + \alpha^2 \langle y'^2 \rangle. \quad (12)$$

If u' and y' are uncorrelated,

$$\langle \hat{u}'^2 \rangle \approx \langle u'^2 \rangle + 2\alpha^2 \langle v'^2 \rangle T_v t, \quad t \gg T_v, \quad (13)$$

where Eq. (6) has been used. Assuming $\langle u'^2 \rangle \sim O(\langle v'^2 \rangle)$,

$$\langle \hat{u}'^2 \rangle \approx \langle u'^2 \rangle, \quad (14)$$

for $t \ll (\alpha^2 T_v)^{-1}$. This time scale can be estimated as follows: east of the Hawaiian Islands, the zonal current is 0 m/s at 26°N and is -0.2 m/s at 14°N, giving $|\alpha| \sim 1.5 \times 10^{-7} \text{ s}^{-1}$. Using this value and $T_v \sim 3.2$ days, $(2\alpha^2 T_v)^{-1} \sim 930$ days. Because we are interested in dispersion for $t \leq 120$ days, we proceed under the assumption that Eq. (14) applies and restrict this derivation to the time range

$$T_u \ll t \ll (2\alpha^2 T_v)^{-1}. \quad (15)$$

The estimated autocorrelation of u' is

$$\begin{aligned} \hat{R}_u &= (\langle u'^2 \rangle T_m)^{-1} \int_0^{T_m} d\tau [u'(t) + \alpha y'(t)] \\ &\quad \times [u'(t + \tau) + \alpha y'(t + \tau)] \\ &\approx R_u + 2\alpha^2 T_v t R_y \langle v'^2 \rangle / \langle u'^2 \rangle, \end{aligned} \quad (16)$$

where R_y is the autocorrelation of $y'(t)$, a function which decays considerably more slowly than R_v . Because $R_y \leq 1$, $t \ll 1/2\alpha^2 T_v$, and $\langle u'^2 \rangle \sim O(\langle v'^2 \rangle)$,

$$\hat{R}_u \approx R_u. \quad (17)$$

The estimated autocorrelation function is not significantly contaminated by the meridional shear in $\langle u \rangle$, so the integral scales should not be either.

The long-time dispersion is

$$\begin{aligned} \langle \hat{x}'^2 \rangle &= 2\langle u'^2 \rangle \int_0^t d\tau (t - \tau) \hat{R}_u(\tau) \\ &\approx 2\langle u'^2 \rangle t \int_0^t d\tau \left[R_u + 2 \frac{\langle v'^2 \rangle}{\langle u'^2 \rangle} \alpha^2 T_v t R_y \right] \\ &= 2\langle u'^2 \rangle T_u t + 4\langle v'^2 \rangle \alpha^2 T_v T_y t^2, \end{aligned} \quad (18)$$

where T_y is the integral time scale of y' (for all 90-day independent drifter segments in the central North Pacific, the mean value of T_y is 11 days). The

second term on the right-hand side of Eq. (18) scales to the first term as

$$\frac{4\langle v'^2 \rangle \alpha^2 T_v T_y t}{\langle u'^2 \rangle T_u} \sim 4\alpha^2 T_y t. \quad (19)$$

Thus, for $t > 1/4\alpha^2 T_y \sim 100$ days, x_{rms} grows linearly due to the meridional shear of the mean zonal current.

According to Eq. (18), the mean shear scales as

$$|\alpha| \sim \frac{dx_{\text{rms}}/dt}{2\sqrt{\langle v'^2 \rangle T_v T_y}}. \quad (20)$$

Thus, an estimate of $|\alpha|$ can be derived from the observed long-time dispersion. From Fig. 4, $\Delta x_{\text{rms}}/\Delta t$ for the east group of drifters between days 100 and 120 is ~ 0.05 m/s. Using this value, $v' \sim 0.11$ m/s, $T_v \sim 5$ days and $T_y \sim 11$ days, Eq. (20) gives $|\alpha| \sim 3.5 \times 10^{-7} \text{ s}^{-1}$, approximately twice the direct measurement ($|\alpha| \approx 1.5 \times 10^{-7} \text{ s}^{-1}$). This discrepancy may be due to the first term in the right-hand side of Eq. (18) playing a non-negligible role. Nevertheless, given the crude scaling arguments involved, this order-of-magnitude agreement suggests that the gyre-scale meridional shear can account for the observed long-time zonal dispersion.

6. Lagrangian spectra

The integral scales presented in this paper are essentially first-moment descriptions of the Lagrangian velocity spectra. They do not, however, give details of the cyclonic/anticyclonic distribution of energy or higher-moment information. In order to examine the mean Lagrangian spectra, we took non-overlapping 120-day segments of the drifter trajectories, removed the mean from the velocity time series, applied a 10% cosine window and calculated the spectra. Individual spectra within a group were used to obtain standard error bars for the mean spectral energy density via bootstrapping.

Fig. 5 shows the variance-preserving spectra of zonal and meridional drifter speed. In the lee gyre, the energetic eddy-containing band is at 3–20 days period. This band shifts to 10–40 days for the other groups north of the North Equatorial Current, and to

20–60 in the NEC. At the lowest resolved frequencies, the zonal component of velocity is more energetic than the meridional component for all groups except the northwest and northeast. Higher-frequency motion (periods smaller than 30–40 days) are everywhere isotropic. The lee gyre spectra are dominated by sharp peaks; the rotary spectra (Fig. 6) show that these peaks are due to single-signed lee vortices. Cyclonic peaks are at 4–6, 8 and 14 days; anticyclonic peaks are at 6, 12 and 22 days, with additional, barely significant peaks at 3 and 7 days. The cyclonic spectrum in the anticyclonic gyre has a peak at 5 days, due to strong lee anticyclones occasionally advecting weaker, wind-generated cyclones southward in the immediate lee of Hawaii.¹ The discretization of eddy energy suggests that the motion is a resonant response to direct forcing, or that some process or combination of processes is quantizing the mesoscale variability within the eddy band (such as vortex generation by shear instability and downstream vortex merging (Flament et al., 2001)). For the northwest and northeast groups, anticyclonic energy is significantly greater than cyclonic energy throughout most of the eddy band. The northwest spectrum also has a prominent anticyclonic peak at 15 days, possibly due to eddy generation at the Subtropical Front (Qiu, 1998).

Log–log plots of the spectra for the zonal/meridional components of velocity are shown in Fig. 7. The spectra of groups north of the North Equatorial Current and east of the Hawaiian Archipelago have a low-frequency energy plateau with a cutoff at 20–30 days, followed by a high-frequency slope of ~ -2 . A similar Lagrangian spectral slope was found by Colin de Verdière (1983), who attributed it to the off-resonance mesoscale response to direct wind forcing. In the North Equatorial Current, the zonal spectrum is red to the lowest resolved frequency. Both NEC spectra have a shallow slope of ~ -1.5 past a cutoff of ~ 40 days, which becomes even shallower at 3–6 days before rapidly dropping at very high frequencies. This weak spectral slope implies that motion at frequencies higher than the

¹ This process has been observed using a synthesis of the drifter trajectories, AVHRR imagery and satellite altimetry by Lumpkin (1998).

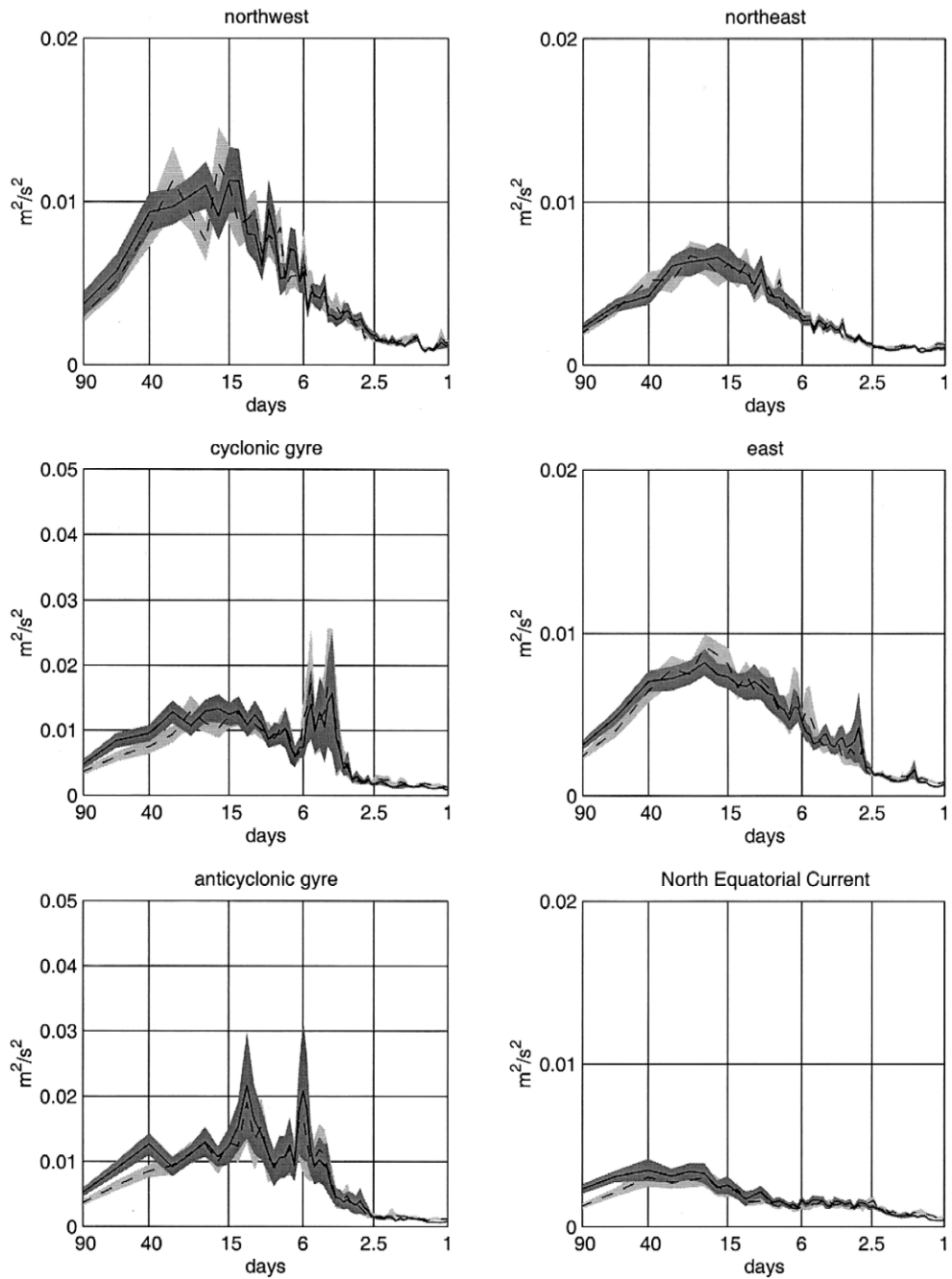


Fig. 5. Variance-preserving plots (frequency times energy density) of the Lagrangian spectra of u (solid, dark shading) and v (dashed, light shading) for the six groups. Shading indicates the standard error bars.

cutoff significantly impact dispersion (Rupolo et al., 1996). The spectra of the lee gyre groups have a

low-frequency cutoff at 40 days, an intermediate slope of ~ -1 from 6–40 days, and a much steeper

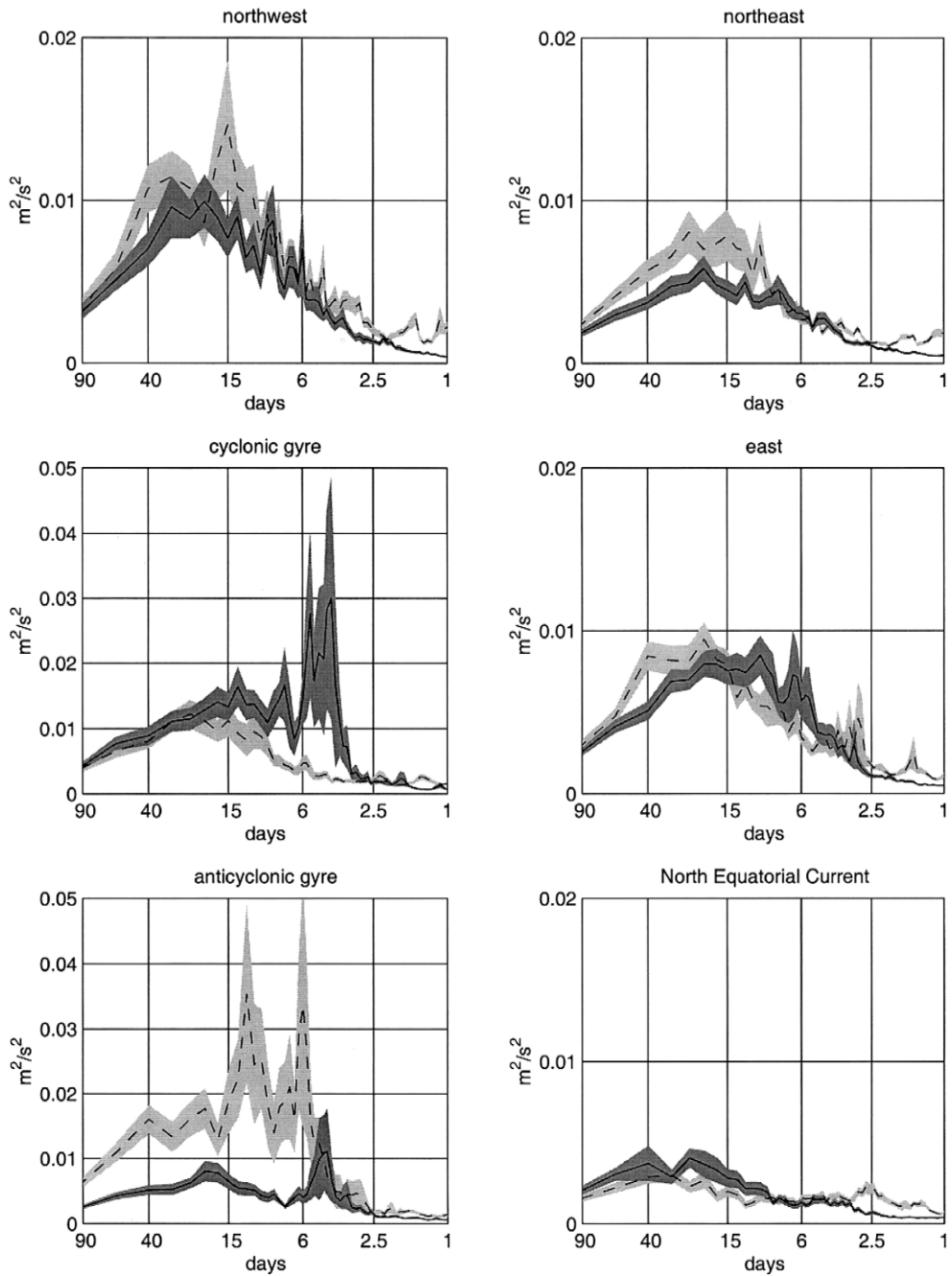


Fig. 6. Variance-preserving plots (frequency times energy density) of the Lagrangian cyclonic (solid, dark shading) and anticyclonic (dashed, light shading) spectra for the six groups. Shading indicates the standard error bars.

high-frequency slope. A similar intermediate power-law regime was discovered in neutrally buoyant float

spectra by Rupolo et al. (1996), who attributed it to the presence of coherent vortices driving anomalous

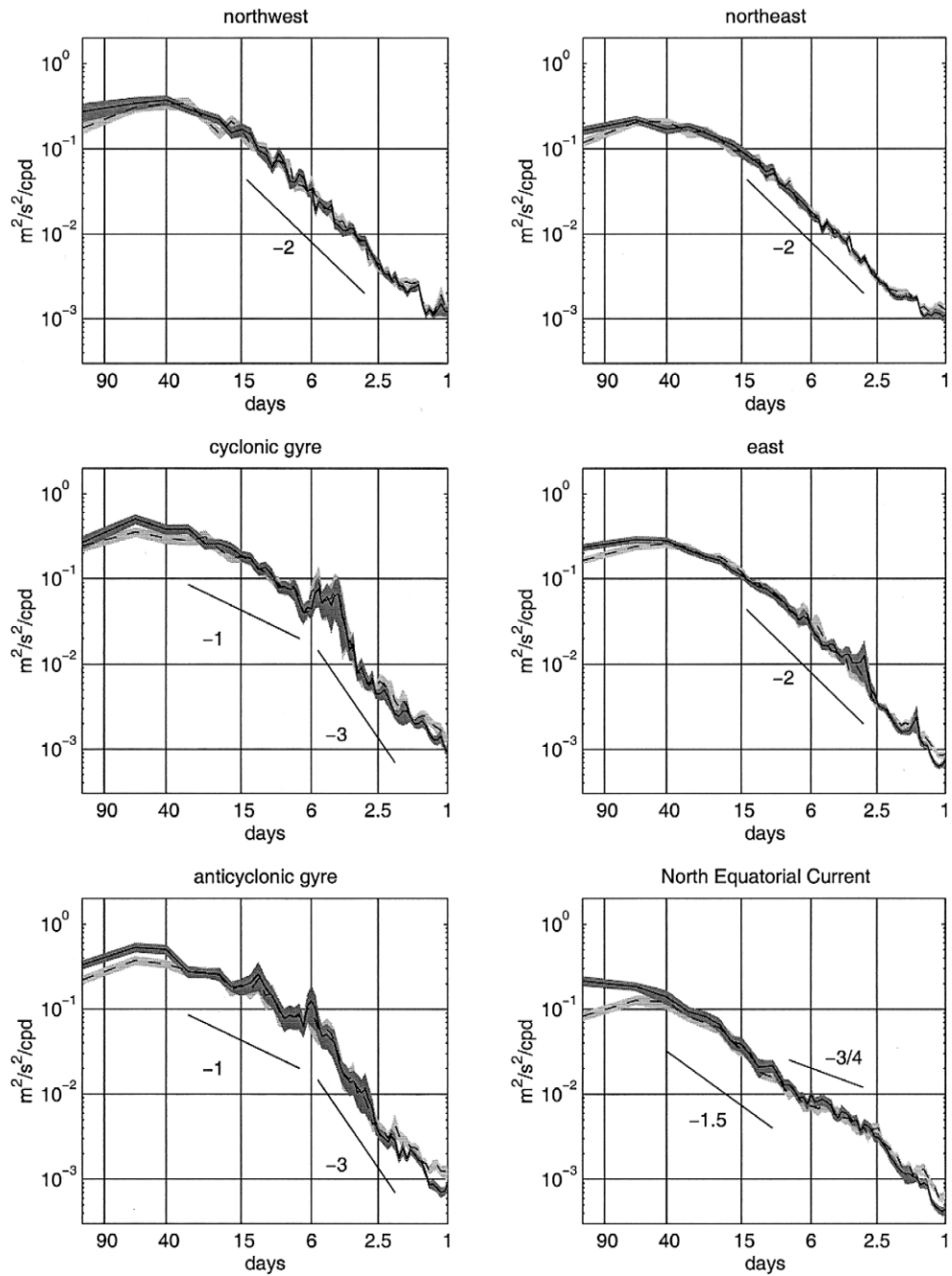


Fig. 7. Log–log plots of the Lagrangian spectra of u (solid, heavy shading) and v (dashed, light shading) for the six groups. Shading indicates the standard error bars.

dispersion over the initial 10 integral time scales. The log–log rotary spectra (Fig. 8) show that the

intermediate regime exists only in the spectra of one sign: the dominant vorticity of that lee gyre. The

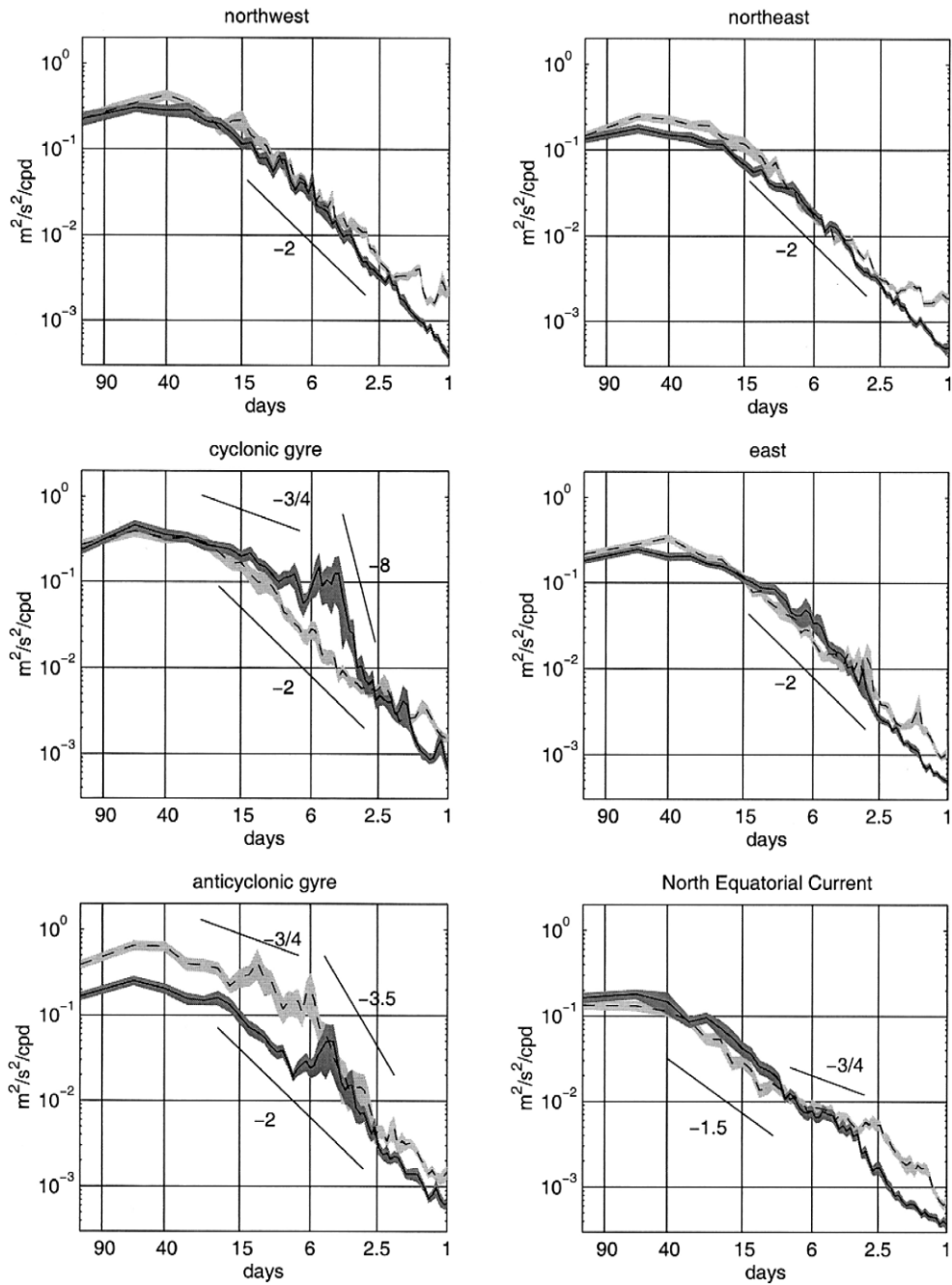


Fig. 8. Log–log plots of the Lagrangian cyclonic (solid, heavy shading) and anticyclonic (dashed, light shading) spectra for the six groups. The shading indicates the standard error bars.

opposite-signed spectra have a -2 slope, similar to those east of Hawaii. Lee vortices create an interme-

diate slope of $\sim -3/4$, with a dropoff steeper than -3 past the high-frequency cutoff.

7. Discussion

Is there a universal empirical law independently relating the length and time scales of eddies to their velocity variance? If so, maps of eddy diffusivity could be constructed directly from maps of eddy kinetic energy (Böning, 1988). Two models have been proposed for this law. Observations of SOFAR floats (700 and 1300 m depth) deployed in MODE and LDE suggest that the Lagrangian scales are related by (Price, in (Rossby et al., 1983; McWilliams et al., 1983)):

$$L_u = u_{\text{rms}} T_u, \quad K_{xx} = u_{\text{rms}}^2 T_u, \quad T_u \text{ constant.} \quad (21)$$

In contrast, Krauss and Böning (1987) found

$$T_u = L_u / u_{\text{rms}}, \quad K_{xx} = u_{\text{rms}} L_u, \quad L_u \text{ constant,} \quad (22)$$

in a study of surface North Atlantic drifters; Brink et al. (1991) found the same relationship applied to drifters in the California Coastal Transition Zone. As noted by Davis (1991), both the length and time scales may change with changing EKE: a tendency for observations to behave more like Eqs. (21) or (22) depends on the relative fluctuation of L_u and T_u . Drifter studies in the California Current system (Poulain and Niiler, 1989; Swenson and Niiler, 1996) have found complementary changes in the two scales with varying u_{rms} such that neither of the two laws is statistically superior. As demonstrated in Fig. 3, the central North Pacific data behave similarly. The zonal length scales are inconsistent with the constant time scale model (Eq. (21)), and both zonal and meridional time scales decrease with increasing eddy speed. However, the meridional length scale increases significantly with eddy speed. Neither model is statistically superior for describing variations in zonal diffusivity as a function of eddy speed. The meridional diffusivity can be matched by the constant time scale model (Eq. (21)) within the error bars, while the constant length scale model (Eq. (22)) cannot.

Within the North Equatorial Current, zonally stretched, highly anisotropic meanders set the dominant scales of oceanic stirring. Higher-frequency, more isotropic eddies determine these scales to the north. In the oceanic wake of the islands, highly energetic and coherent lee vortices magnify the EKE

levels and diffusivities, and create relatively narrow peaks in the rotary spectra. Except in the North Equatorial Current, dispersion is initially ballistic. Over at least 120 days, the meridional dispersion remains consistent with Taylor's Theorem, changing from ballistic to random-walk dispersion which can be characterized by a constant eddy diffusivity set by the integral scales and rms eddy speed. The meridional dispersion, thus, does not appear to be inhibited by conservation of planetary vorticity (O'Dwyer et al., 2000), which should be anticipated when rms meridional displacement has reached

$$L \sim \sqrt{U/\beta} \sim \sqrt{0.15 \text{ m/s}/10^{-11} \text{ m}^{-1} \text{ s}^{-1}} \sim 150 \text{ km,}$$

$$T \sim \sqrt{U\beta}^{-1} \sim 12 \text{ days.}$$

Zonal dispersion is considerably faster than meridional dispersion, and is not consistent with Taylor's Theorem for a homogeneous flow in the long-time random-walk limit. This is an ubiquitous result in open-ocean drifter studies, attributed to topographic effects (Rossby et al., 1975; Freeland et al., 1975), spatial anisotropy of meanders (Colin de Verdière, 1983; Krauss and Böning, 1987), the β -effect (Haidvogel and Keffer, 1984), and meridional shear in the mean zonal flow (Krauss and Böning, 1987). The final hypothesis is consistent with the observed shear of the North Pacific Subtropical Gyre. Zonal eddy diffusivities constructed from the integral scales do not represent an asymptotic limit to the observed growth rate of dispersion.

Calculating eddy diffusivities has become a tradition in drifter studies, and in some circumstances the diffusion model may indeed describe the dispersion of passive tracers. In the presence of a red cascade of eddy energy, however, such diffusivities can be a misleading way of closing the momentum equations. For example, an explicit calculation of Reynolds stress in the wake of the Hawaiian Islands reveals an eddy-to-mean eastward momentum flux convergence at the latitude of the Hawaiian Lee Countercurrent (19–20°N) (Lumpkin, 1998). Given the presence of such a “negative eddy diffusivity,” we advise the reader to approach traditionally computed eddy diffusivities, such as the ones presented here, with caution!

Acknowledgements

We thank Capt. Brainard and the crew of the R.V. Townsend Cromwell, Guy and Dominique of the yacht Touaou, and Pierre and Minouche of the yacht Meranda for their help deploying the drifters. We thank other investigators whose drifters, initially deployed of California or in the equatorial Pacific, eventually reached our area. They generously made the data available through the WOCE and TOGA databases. J. Firing, S. Kennan, M. Pazos, M. Sawyer, C. Lumpkin and D. Young assisted with data collection and processing. This work was supported by the United States Office of Naval Research (Grant #N000149710147), the National Atmospheric and Oceanographic Administration (Joint Institute for Marine and Atmospheric Research, Grant #NA67RJ0154) and our host institutions. Contribution number 5077 of the School of Ocean and Earth Science and Technology, and JIMAR contribution number 00-333.

References

- Batchelor, G.K., 1949. Diffusion in a field of homogeneous turbulence: I. Eulerian analysis. *Aust. J. Sci. Res., Ser. A*, 2, 437–450.
- Böning, C., 1988. Characteristics of particle dispersion in the North Atlantic: an alternative interpretation of SOFAR float results. *Deep-Sea Res.* 35, 1379–1385.
- Brink, K.H., Beardsley, R.C., Niiler, P.P., Abbott, M., Huyer, A., Ramp, S., Stanton, T., Stuart, D., 1991. Statistical properties of near-surface flow in the California coastal transition zone. *J. Geophys. Res.* 96, 14693–14706.
- Chassignet, E.P., Cushman-Roisin, B., 1991. On the influence of a lower layer on the propagation of nonlinear oceanic eddies. *J. Phys. Oceanogr.* 21, 939–957.
- Colin de Verdière, A., 1983. Lagrangian eddy statistics from surface drifters in the eastern North Atlantic. *J. Mar. Res.* 41, 375–398.
- Davis, R., 1982. On relating Eulerian and Lagrangian velocity statistics: single particles in homogeneous flows. *J. Fluid Mech.* 114, 1–26.
- Davis, R.E., 1991. Observing the general circulation with floats. *Deep-Sea Res.* 38, S531–S571.
- Flament, P., Lumpkin, R., Tournadre, J., Armi, L., 2001. Vortex pairing in an unstable anticyclonic shear flow: discrete subharmonics of one pendulum day. *J. Fluid Mech.*, submitted for publication.
- Freeland, H.J., Rhines, P.B., Rossby, T., 1975. Statistical observations of the trajectories of neutrally buoyant floats in the North Atlantic. *J. Mar. Res.* 33, 383–404.
- Haidvogel, D.B., Keffer, T., 1984. Tracer dispersal by mid-ocean eddies. *Dyn. Atmos. Oceans* 8, 1–40.
- Hansen, D.V., Poulain, P.-M., 1996. Quality control and interpolations of WOCE–TOGA drifter data. *J. Atmos. Oceanogr. Tech.* 13, 900–909.
- Krauss, W., Böning, C.W., 1987. Lagrangian properties of eddy fields in the northern North Atlantic as deduced from satellite-tracked buoys. *J. Mar. Res.* 45, 259–291.
- Lumpkin, C., 1998. Eddies and Currents of the Hawaiian Islands. PhD dissertation, School of Ocean and Earth Sciences and Technology, University of Hawaii at Manoa.
- McWilliams, J., Brown, E., Bryden, H., Ebbesmeyer, C., Elliot, B., Heinmiller, R., Hua, B.L., Leaman, K., Lindstrom, E., Luyten, J., McDowell, S., Owens, W.B., Perkins, H., Price, J., Regier, L., Riser, S., Rossby, H., Sanford, T., Shien, C., Taft, B., Leer, J.V., 1983. The local dynamics of eddies in the western North Atlantic. In: Robinson, A. (Ed.), *Eddies in Marine Science*. Springer-Verlag, Berlin, pp. 92–113.
- O'Dwyer, J., Williams, R.G., LaCasce, J.H., Speer, K.G., 2000. Does the potential vorticity distribution constrain the spreading of floats in the North Atlantic? *J. Phys. Oceanogr.* 30, 721–732.
- Paduan, J.D., Niiler, P.P., 1993. Structure of velocity and temperature in the northeast Pacific as measured with Lagrangian drifters in Fall 1987. *J. Phys. Oceanogr.* 23, 585–600.
- Patzert, W.C., 1969. Eddies in Hawaiian waters. Technical Report 69-8, Hawaiian Institute of Geophysics, University of Hawaii at Manoa.
- Poulain, P.-M., Niiler, P.P., 1989. Statistical analysis of the surface circulation in the California current system using satellite-tracked drifters. *J. Phys. Oceanogr.* 19, 1588–1603.
- Qiu, B., 1998. Seasonal eddy field modulation of the North Pacific Subtropical Countercurrent: TOPEX/POSEIDON observations and theory. *J. Phys. Oceanogr.* 29, 2471–2486.
- Rossby, T., Voorhis, A.D., Webb, D., 1975. A quasi-Lagrangian study of mid-ocean variability using long range SOFAR floats. *J. Mar. Res.* 33, 355–382.
- Rossby, H.T., Riser, S.C., Mariano, A.J., 1983. The western North Atlantic—a Lagrangian viewpoint. In: Robinson, A. (Ed.), *Eddies in Marine Science*. Springer-Verlag, Berlin.
- Rupolo, V., Hua, B.L., Provenzale, A., Artale, V., 1996. Lagrangian velocity spectra at 700 m in the western North Atlantic. *J. Phys. Oceanogr.* 26, 1591–1607.
- Stammer, D., 1997. Global characteristics of ocean variability estimated from regional TOPEX/POSEIDON altimeter measurements. *J. Phys. Oceanogr.* 27, 1743–1769.
- Swenson, M.S., Niiler, P.P., 1996. Statistical analysis of the surface circulation of the California Current. *J. Geophys. Res.* 101, 22631–22645.
- Taylor, G.I., 1921. Diffusion by continuous movements. *Proc. London Math. Soc.* 20, 196–212.